Catalysis
Science & Technology

Cite this: *Catal. Sci. Technol.*, 2011, **1**, 740–746

www.rsc.org/catalysis

PAPER

Synthesis of high surface area $CuMn_2O_4$ by supercritical anti-solvent precipitation for the oxidation of CO at ambient temperature

Z.-R. Tang,[a] S. A. Kondrat,[a] C. Dickinson,[b] J. K. Bartley,[a] A. F. Carley,[a] S. H. Taylor,[a] T. E. Davies,[a] M. Allix,[b] M. J. Rosseinsky,[b] J. B. Claridge,[b] Z. Xu,[b] S. Romani,[b] M. J. Crudace[c] and G. J. Hutchings*[a]

Received 25th February 2011, Accepted 9th May 2011
DOI: 10.1039/c1cy00064k

A series of high surface area nanocrystalline copper manganese oxide catalysts have been prepared by supercritical anti-solvent (SAS) precipitation using CO_2 and tested for the ambient temperature oxidation of CO. The catalysts were prepared by precipitation from an ethanol/metal acetate solution and the addition of small quantities of water was found to result in a mixed acetate precursor with surface areas >200 m^2 g^{-1}, considerably higher than those prepared by conventional precipitation methods. The surface area of the final calcined mixed oxide was found to be dependent upon the initial water concentration. XRD and FT-IR analysis indicated that the addition of water promoted the formation of carbonate species in the amorphous acetate precursor, with high resolution TEM and STEM showing the material to consist of spherical agglomerations of fibrous strings of *ca.* 30 nm length. This is in contrast to the material prepared in the absence of water, using the same SAS methodology, which typically yields quasi-spherical particles of 100 nm size.

Introduction

The synthesis of a catalytic material and indeed any chemical product using sustainable and green methods is the subject of considerable interest. In many cases the use of certain organic solvents, especially chlorinated hydrocarbons, as well as the nitrate intermediates (often used in commercial catalyst syntheses) mean that there is need for post treatment of hazardous effluent which is both environmentally and economically unsound. Indeed, green or sustainable chemistry applies the principle that it is better not to generate the waste in the first place rather than treating and disposing of it afterwards. In 2005 Noyori identified three key developments in green chemistry; (1) the use of supercritical carbon dioxide as a solvent; (2) the use of aqueous hydrogen peroxide for oxidation reactions and (3) the use of asymmetric hydrogenation in organic synthesis.[1] The synthesis and processing of novel materials *via* either supercritical anti-solvent precipitation (SAS), gas anti-solvent precipitation (GAS) or rapid expansion of an anti-solvent solution (RESS) has received considerable attention in recent years and has proven to be a viable process utilised in many areas including chemical synthesis, particle generation, extraction and material processing.[2–6] There has been extensive research into the processes for the synthesis of semiconductors, polymers, pharmaceuticals and explosives,[7–14] but little attention has been paid to the synthesis of catalytic materials. Previously, we have shown how SAS processing can be successfully applied to the synthesis of vanadium phosphates for the conversion of n-butane to maleic anhydride,[15–17] as well as the generation of high surface area supports suitable for oxidation reactions.[18–20] Crucially, these materials displayed novel properties intrinsic to this unique method of synthesis which is vital if is this method of materials synthesis is to be considered as advantageous over traditional routes.

Recently we have shown how copper manganese oxide prepared by the SAS process can be highly active for the conversion of CO to CO_2, highlighting how the intimate mixing afforded by the method resulted in a highly homogeneous mixed metal oxide.[21] Comparison with a commercial copper manganese oxide catalyst showed that the material prepared using SAS precipitation was intrinsically more active, although the low surface area of the material limited its applicability.

Copper manganese oxide has been known to be active for the conversion of CO to CO_2 for over a hundred years and although a number of more active materials have been discovered since, especially those based on precious metals,[22,23] economic reasons have meant that hopcalite, amorphous $CuMn_2O_4$, is still the commercial catalyst of choice. The precise mechanism for the CO conversion has eluded researchers for years but

[a] *Cardiff Catalysis Institute, School of Chemistry, Cardiff University, Main Building, Park Place, Cardiff, CF10 3AT, UK*
[b] *Department of Chemistry, University of Liverpool, Crown Street, Liverpool, L69 7ZD, UK*
[c] *Molecular Products Limited, Mill End, Thaxted, Essex, CM6 2LT, UK*

there is a general consensus in the literature that activity is related to the redox couple at specific sites on the surface of the catalyst:[24,25]

$$Cu^{2+} + Mn^{3+} \rightarrow Cu^{+} + Mn^{4+}$$

Deactivation is considered to occur when the catalyst is heated above the crystallization point of 350 °C where crystalline $CuMn_2O_4$, $CuMnO_2$ and Mn_3O_4 form.[25]

A number of studies have looked into novel methods of hopcalite synthesis with varying degrees of success. Rangappa and co-workers have synthesised high surface area copper manganese oxide using supercritical water[26] whereas Krämer *et al*. have shown that sol–gel preparation routes with ethylene glycol can result in high surface area materials with activity comparable to commercial hopcalite.[27]

The activity of hopcalite also depends on its morphology since many studies have shown that hopcalite is highly active in the amorphous state[24,27,28] even at room temperature, and the activity is lost if the material is calcined at temperatures above *ca*. 500 °C when the crystalline spinel phase is formed. Studies of the synthesis methods indicated that the activity of hopcalite is known to depend on the structure of the catalyst precursor[29] and in general this is controlled by the preparation method. We have previously investigated the effect of stoichiometry and the co-precipitation parameters on catalyst performance[30,31] and demonstrated that the ageing time during which the co-precipitated composition ripens before it is separated and dried is of crucial importance. In the preparation of active hopcalite catalysts the most active catalysts were the stoichiometric $CuMn_2O_4$ prepared with a 12 h aging step. This modified approach has led to the preparation of hopcalite with significantly improved catalytic activity.

It is well known that active hopcalites are currently prepared by co-precipitation of a basic carbonate from a solution of the nitrates using sodium carbonate. Using supercritical fluids in catalyst preparation provides one possibility of a nitrate-free path to catalysts and catalyst precursors, thereby providing a new route for catalyst manufacture.

In the present study we have focused on the preparation of nanostructured CuMnOx using supercritical CO_2 as an anti-solvent and acetates as starting precursors. Different solvents for metal acetates including pure solvents and co-solvents containing water have been investigated and catalysts with high activity for CO oxidation at room temperature have been obtained.

2. Experimental

2.1 Catalyst preparation

A mixed solution of copper acetate (0.005 mol, Aldrich) and manganese acetate (0.01 mol, Aldrich) was prepared in H_2O/ethanol in which the H_2O concentration varied from 0–100 vol% and processed using supercritical CO_2. The apparatus used has been described previously.[16] The liquefied CO_2 was pumped (Jasco PU-1580-CO_2) up to 110 bar (7 ml min^{-1}) and allowed to stabilise (30 min). The pressure in the system was maintained using a back pressure regulator (Jasco BP-1580-81). The precipitation vessel was maintained at 40 °C within an oven. A pure solution of water/ethanol (0–15 vol%) was then pumped (Jasco HPLC PU-980) co-currently for *ca*. 30 min with a co-axial nozzle for the simultaneous delivery of both the CO_2 and solvent/solute mixture prior to introduction of the metal acetate solution. After stabilisation the mixed metal acetate solution was pumped into the system (0.1 ml min^{-1}). The system was run for 16 h resulting in a typical yield of approximately 0.5 g. The precursor material was then calcined (300 °C, 2 h, 10 °C min^{-1}) to give the final catalyst.

2.2 Catalyst characterisation

X-Ray diffraction analysis was performed on an Enraf Nonius FRS90 X-ray generator with a Cu-Kα source fitted with an Inel CPS 120° position sensitive detector. Surface area analysis was determined by nitrogen adsorption at −196 °C using a Micromeretics Gemini 2360 according to the Brauner Emmet Teller method. All samples were degassed under N_2 for 2 h at 110 °C prior to analysis. Thermo-gravimetric analysis (TGA) was performed using a Setaram Labsys TG-DTA/DSC 1600 instrument. Fourier transform-infrared (FT-IR) spectra were recorded on a Perkin Elmer series 2000 FT-IR spectrometer with the sample pressed into KBr discs. Scanning electron microscopy (SEM) was performed using a Hitachi S-2460N microscope. Samples were coated with gold prior to analysis.

Samples for scanning transmission electron microscopy (STEM) and transmission electron microscopy (TEM) examination were prepared by dispersing the catalyst powder in high purity ethanol, then allowing a drop of the suspension to evaporate on a holey carbon microscope grid. Lattice imaging in both bright field (BF) and high angle annular dark field (HAADF) were carried out on a 3rd ordered spherical aberration corrected VG HB 501 with a Nion Mark II Quadropole-Octupole STEM (SuperSTEM) operating at 100 kV. The spatial resolution for the HAADF is ∼1 Å. Samples were also subjected to chemical microanalysis in a VG HB601 UX STEM operating at 100 kV. This microscope was fitted with an Oxford Instruments INCA TEM 300 system for energy dispersive X-ray (EDX) analysis. TEM images were taken on a JEOL 300 kV JEM3010 with LaB_6 filament.

2.3 Catalyst testing

CO oxidation experiments were conducted on 50 mg of samples in a fixed bed microreactor. Sample was secured between quartz wool in a glass u-tube and the temperature isothermally maintained at 25 °C using a water bath. The space velocity was typically 12 000 h^{-1} using a premixed cylinder (5000 ppm CO in synthetic air, British Oxygen Company). Product analysis was performed using on-line gas chromatography.

3. Results and discussion

In an effort to probe the effects of water addition on the structure and activity of copper manganese oxides a series of catalysts were synthesised by SAS using supercritical CO_2 ($scCO_2$) with various concentrations of water in the initial ethanol mixed metal acetate solution. Previously, we have shown how copper manganese oxide prepared by SAS using

Table 1 BET surface areas of the materials prepared by SAS precipitation with different solvent mixtures

Water content (vol%)	Precursor (m^2 g^{-1})	Calcined 300 °C 2 h (m^2 g^{-1})
0	264	33
5	200	65
10	152	136
15	140	175

supercritical CO_2 with DMSO as solvent gave rise to highly active catalysts for CO oxidation, but the overall activity was limited by the low surface area of the material.[21] The exothermic nature of the acetate decomposition combined with the higher calcination temperatures required for complete removal of residual solvent resulted in structural instability, sintering and gave a final catalyst with surface areas of approximately 10–50 m^2 g^{-1}. Also, the use of less toxic solvents such as ethanol and methanol are preferred over the more toxic and environmentally unsound DMSO. BET surface areas of the as prepared mixed metal acetates are presented in Table 1. It should be stated that although concentrations ranging from 0–100 vol% water were tested it was found that no product was obtained with water concentrations higher than 15 vol% due to the poor miscibility of $scCO_2$ in water lowering the anti-solvent properties of $scCO_2$. What is immediately apparent is the remarkably high surface area of the precursor material prepared using ethanol in the SAS process. Table 1 shows how preparation with pure ethanol results in a precursor surface area of 264 m^2 g^{-1}. This decreases with increasing water content to 140 m^2 g^{-1} at 15 vol% but is still significant. The decrease in surface area with increasing water content is consistent with the reduced miscibility of CO_2 in water. It should also be noted that upon calcination the surface areas of the 0–10 vol% H_2O are observed to decrease, whereas the 15 vol% H_2O/CuMnOx increases from 140 to 175 m^2 g^{-1}. These surface areas are far higher than the 23–31 m^2 g^{-1} reported by Mirzaei *et al.*,[30] 35 m^2 g^{-1} reported by Wright *et al.*[28] and the 27 m^2 g^{-1} reported by Porta *et al.*[32]

Analysis of the precursor material by XRD indicated that the addition of water promoted the formation of crystalline carbonate species (Fig. 1), with the main phases attributed to $MnCO_3$. With no water present, the precursor is highly amorphous, but becomes increasingly crystalline as the concentration of water increases which is consistent with the decrease in surface area. The main phase present was identified as rhodochrosite ($MnCO_3$ XRD reflections at 24.3, 31.5, 38.1, 41.8, 45.3, 51.9 degrees 2θ). No copper containing phases are observed in the diffractograms. The structure of the catalyst precursor is known to have a profound effect upon the activity of the final catalyst with Porta *et al.* highlighting the importance of the presence of hydroxycarbonates.[32] It is proposed that in the process studied here, the addition of water promotes the formation of carbonic acid during the precipitation giving rise to carbonates as opposed to acetates.

Calcination of the precursor at 300 °C for 2 h (Fig. 2) resulted in the formation of $Cu_{1.5}Mn_{1.5}O_4$ (XRD reflections at 30.6, 36.1, 38.8, 43.6, 57.8, 63.7 degrees 2θ), the crystallinity of which decreased with increasing water concentration. Interestingly, the more crystalline precursors gave a more amorphous catalyst as decomposition of the higher concentrations of carbonate

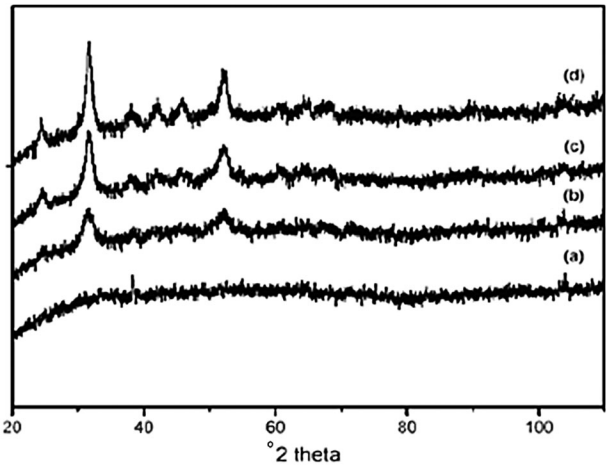

Fig. 1 XRD patterns of the precursors formed with different solvent mixtures: (a) 0 vol% H_2O/EtOH (b) 5 vol% H_2O/EtOH (c) 10 vol% H_2O/EtOH (d) 15 vol% H_2O/EtOH.

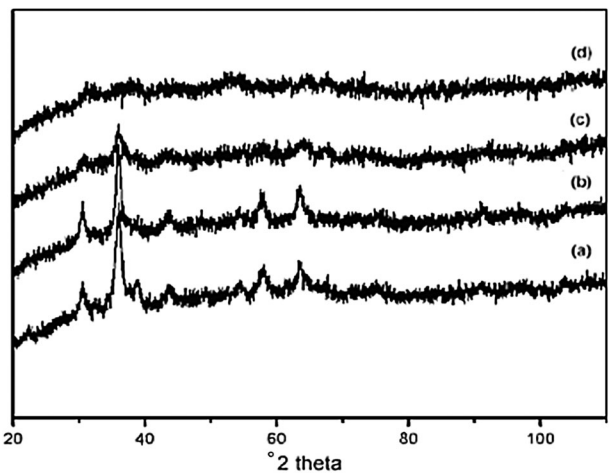

Fig. 2 XRD patterns of the precursors formed with different solvent mixtures calcined at 300 °C: (a) 0 vol% H_2O/EtOH (b) 5 vol% H_2O/EtOH (c) 10 vol% H_2O/EtOH (d) 15 vol% H_2O/EtOH.

became more difficult at 300 °C. Previously, Hutchings *et al.* demonstrated how amorphous materials comprising predominantly stoichiometric $CuMn_2O_4$ phases along with Mn_2O_3 and CuO are considerably more active than other materials.[33] TGA analysis of the precursor material prepared with pure ethanol is shown in Fig. 3a. The precursor displays a four stage weight loss with the first weight loss <100 °C attributed to residual solvent. The second weight loss at approximately 200 °C is indicative of copper hydroxide decomposition with the final weight losses at 236 and 297 °C attributed to the decomposition of copper acetate

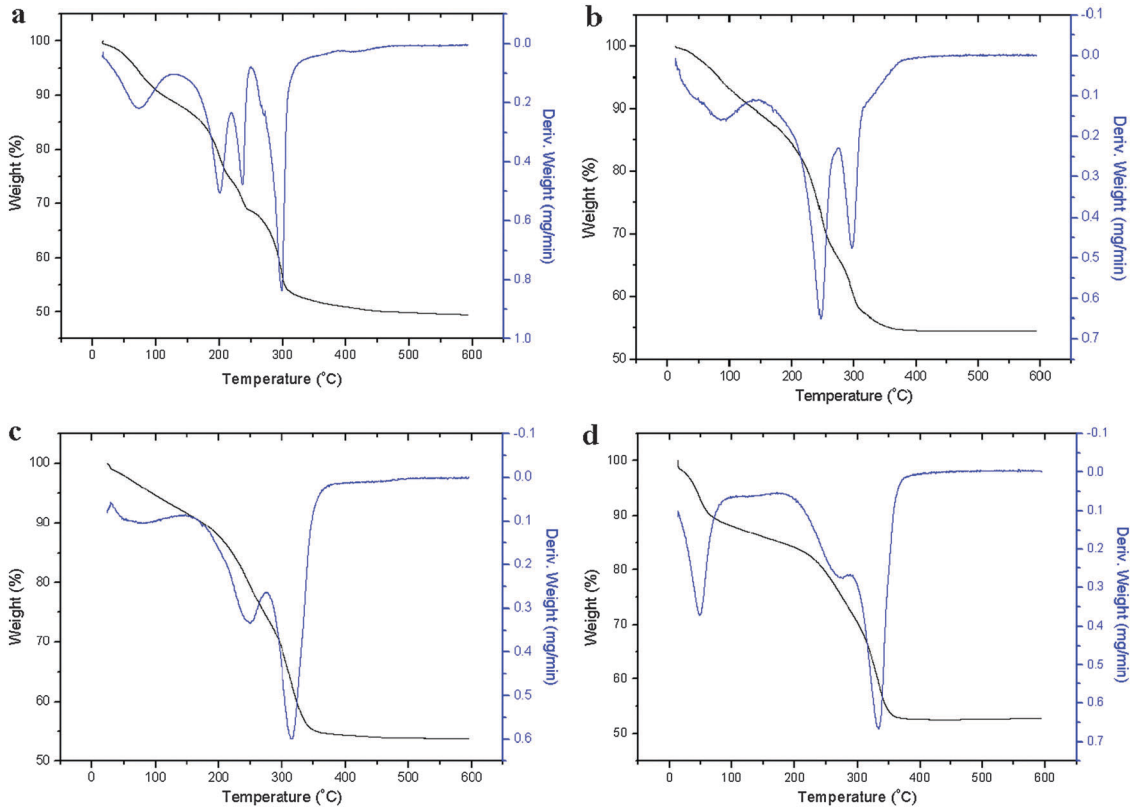

Fig. 3 TGA analysis of the precursors formed with different solvent mixtures: (a) 0 vol% H_2O/EtOH (b) 5 vol% H_2O/EtOH (c) 10 vol% H_2O/EtOH (d) 15 vol%H_2O/EtOH.

and manganese acetate respectively. With the increase in the water concentration the decomposition pattern changes as the carbonate species becomes dominant. Only three significant weight losses are apparent for the materials prepared with water present and these are attributed to the loss of physically adsorbed solvent (< 100 °C), mixed copper acetate and carbonate (*ca.* 250 °C) and manganese acetate and carbonate (*ca.* 300 °C). Increasing the water concentration to 15 vol% resulted in the almost exclusive formation of carbonates, highlighted by the shift in the temperature of the weight losses from 245 to 269 °C and from 297 to 332 °C for the second and third decomposition steps respectively. This increase in the amount of carbonates present is confirmed by both the XRD and FT-IR analysis as shown in Fig. 4.

FT-IR analysis of the sample prepared with pure ethanol confirmed the presence of metal acetate salts, demonstrated by the main bands at 1561 and 1481 cm^{-1}. As the water content of the initial solvent mixture increases, the intensity of these bands decreases and the formation of the carbonate species is observed from the bands at 1485 and 862 cm^{-1}.

CO oxidation activity for the calcined catalyst has been determined and is presented in Fig. 5. From the results, a number of important conclusions may be drawn. Firstly it is apparent that the catalytic activity is enhanced when using water as a co-solvent. Secondly, the most active catalyst is that prepared using 10 vol% H_2O/ethanol with activity decreasing dramatically with a modest increase in the water concentration to 15 vol%. It is evident that the presence of water has a profound effect on the chemistry, with minor concentration

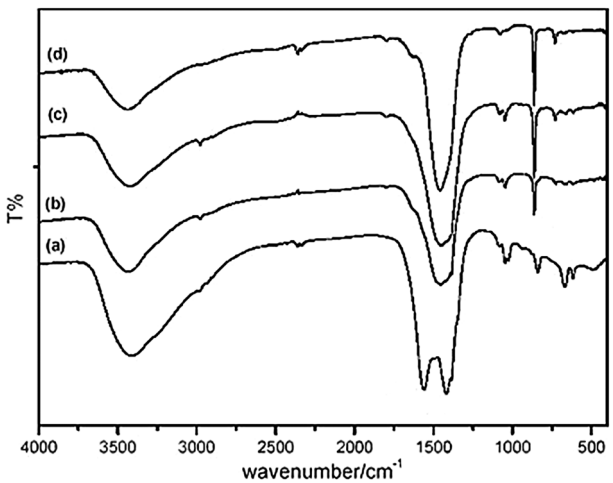

Fig. 4 FT-IR spectra of the precursors formed with different solvent mixtures: (a) 0 vol% H_2O/EtOH (b) 5 vol% H_2O/EtOH (c) 10 vol% H_2O/EtOH (d) 15 vol% H_2O/EtOH.

variations giving rise to major differences in the catalytic activity. The pattern of activity with time-on-line is interesting as it shows a high initial activity which drops off rapidly after *ca.* 20 min. A similar pattern is observed with precious metal catalysts prepared using standard co-precipitation.[18]

Scanning electron micrographs (Fig. 6) highlight the differences between precursors and final catalysts after calcination, as well as the differences between materials made with and without water as co-solvent. It was observed that the

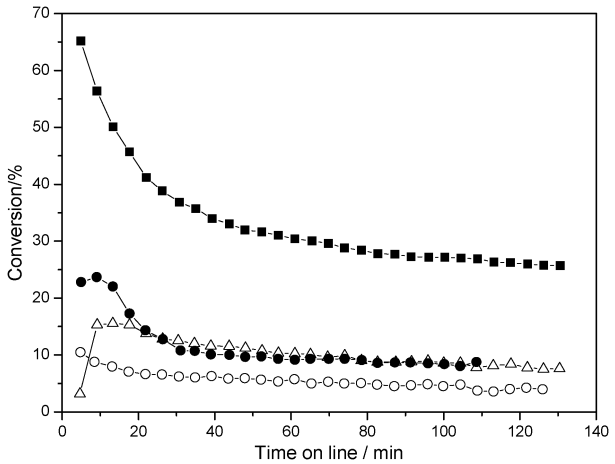

Fig. 5 Conversion of CO at 25 °C with time-on-line (5000 ppm CO, GHSV 12 000 h^{-1}). Water co-solvent concentration: (○) 0 vol% H_2O/EtOH (△) 5 vol% H_2O/EtOH (■) 10 vol% H_2O/EtOH (●) 15 vol% H_2O/EtOH.

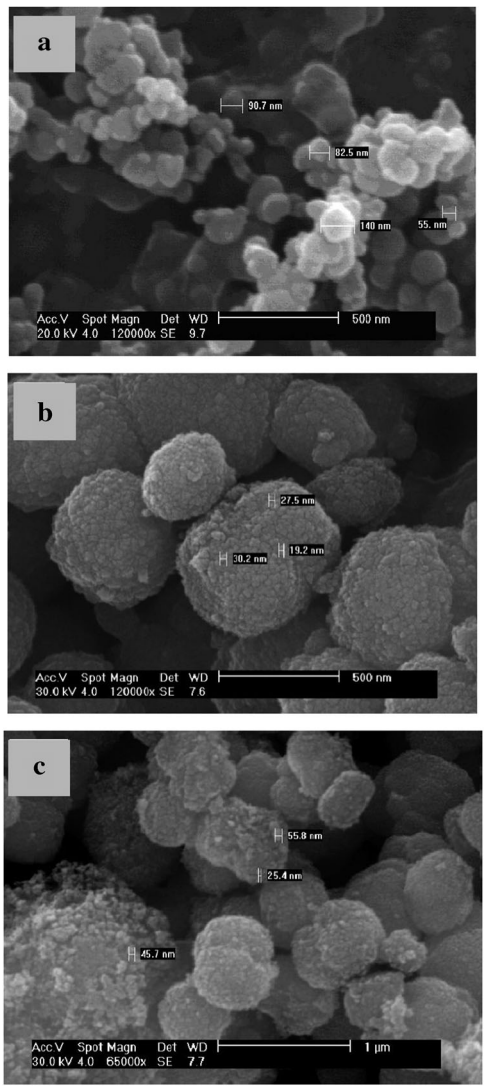

Fig. 6 SEM images of: (a) 0 vol% H_2O/EtOH precursor, (b) 10 vol% H_2O/EtOH precursor and (c) 10 vol% H_2O/EtOH calcined catalyst.

material formed without water present (Fig. 6a) had particles of a quasi-spherical morphology, with sizes ranging from 50 to 150 nm that tended to aggregate into clusters. In the presence of water (Fig. 6b), larger spherical particles ranging from 350 nm to >1 µm were observed. Upon higher magnification, these larger spherical particles were found to comprise aggregates of smaller (~20–30 nm) sized particles.

The observable change in morphology with the addition of water indicates a change in the precipitation mechanism. The small quasi-spherical morphology formed in the pure ethanol system is consistent with materials produced in a surface tension free environment. The lack of surface tension has been reported in SAS precipitations in which the system is above the mixed critical point, with the solvent and the CO_2 anti-solvent being completely miscible.[34] The addition of water to the system reduces the miscibility of solvent and anti-solvent which results in the presence of surface tension between the solution droplet and the CO_2. Consequently, a conventional diffusion based mechanism would predominate, with CO_2 diffusing into the droplet and resulting in the formation of the observed agglomerates. The morphology of the precursors did not significantly alter on calcination with the only change observed being a partial breakdown of the spherical agglomerates. Fig. 7 shows TEM images of calcined catalysts precipitated using 10 vol% H_2O in ethanol, along with that of a sample formed using 100% ethanol. As observed previously, particles formed without water as co-solvent are quasi-spherical and are approximately 100 nm in size. Particles formed with the addition of water are small fibres with dimensions of 30 by <5 nm, and these aggregate to form the larger spherical particles seen in the SEM images.

High resolution TEM of the catalyst samples (Fig. 8), indicate that the calcined material from the 10 vol% H_2O in ethanol precipitation were predominantly amorphous with small areas of crystalline material. STEM analysis indicated that the samples formed with 10 vol% H_2O in ethanol comprise predominantly homogeneous and intimately mixed

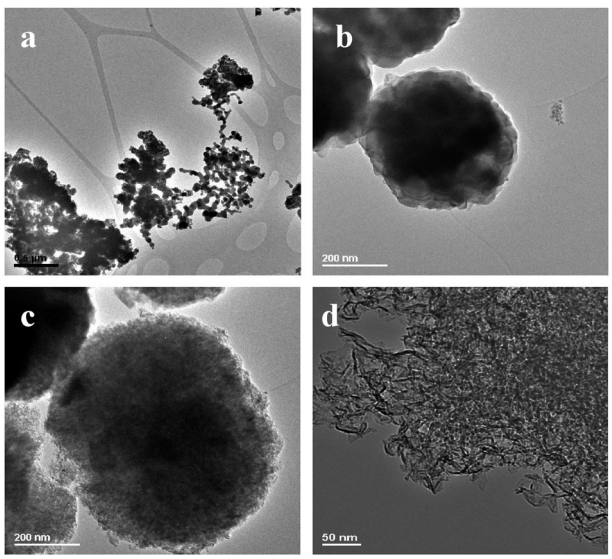

Fig. 7 TEM images of calcined catalysts prepared with (a) 0 vol% H_2O/ethanol (b–d) 10 vol% H_2O/ethanol.

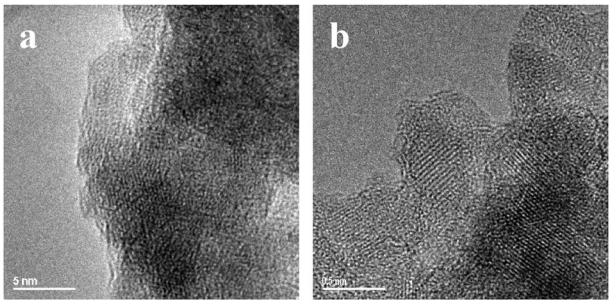

Fig. 8 HRTEM images of the calcined catalysts prepared with 10 vol% H_2O/EtOH showing (a) amorphous and (b) small crystallites in amorphous material.

copper/manganese phases. A small degree of phase separation was observed (Fig. 9), with greater degrees of separation being observed in the less active catalysts. This indicates that a diffusion based mechanism proceeds with the addition of water, which results in a more phase separated catalyst precursor and subsequent catalyst. Greater volumes of water in the system led to further reductions in CO_2-solvent miscibility and therefore, greater phase separation. Therefore, the addition of water co-solvent in the SAS precipitation resulted in an alteration of the composition of both the precursor and the final catalyst. The addition of water resulted in the retention of particle surface area upon calcination due to the formation of carbonate precursors as opposed to the acetate materials obtained with pure ethanol.

Conclusions

High surface area nanocrystalline copper manganese oxide catalysts have been successfully prepared using SAS precipitation with $scCO_2$ using ethanol/water mixtures as solvent. These catalysts have improved surface areas and are active for CO oxidation. The inclusion of water in the precursor solution resulted in the formation of metal carbonate species which upon calcination gave active catalysts with surface areas in the range 65–175 $m^2\ g^{-1}$. XRD and FT-IR analysis showed the precursor comprised mixed copper manganese carbonate phases; the concentration of which increased with increasing water content to 15% by volume. Detailed TEM analysis indicated that the components were intimately mixed, but the addition of water led to a degree of phase separation due to the poor miscibility of supercritical CO_2 and water. The optimum composition of water in the system is a balance between increased carbonate composition at higher volumes and the greater degree of copper and manganese mixing at lower volumes. We have not attempted to optimise the reaction conditions and hence, by appropriate manipulation of the preparation conditions further enhancement in activity can be expected.

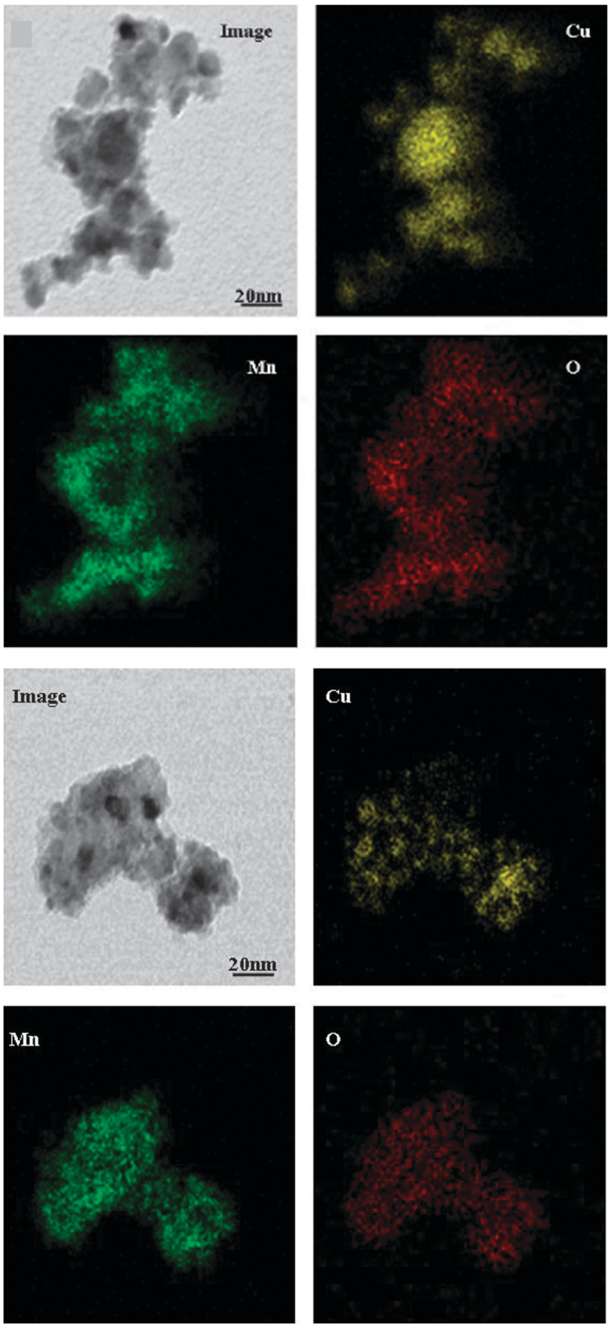

Fig. 9 STEM X-ray energy-dispersive spectrometry (EDS) high resolution mapping of (a) 10 vol% H_2O/EtOH CuMnOx precursor and (b) 10 vol% H_2O/EtOH CuMnOx calcined catalyst showing phase separation.

Acknowledgements

The authors gratefully acknowledge financial support from the EPSRC, the Cardiff Partnership Fund and Molecular Products Limited. We also thank Dr A. Papworth (Department of Engineering, University of Liverpool) for assistance with the STEM measurements and Dr Andrew Bleloch's group (Department of Engineering, University of Liverpool) for assistance with the SuperSTEM measurements.

References

1 R. Noyori, *Chem. Commun.*, 2005, 1807.
2 F. Cansell, C. Aymonier and A. Loppinet-Serani, *Curr. Opin. Solid State Mater. Sci.*, 2003, **7**, 331–340.
3 M. B. King and T. Bott, *Extraction of Natural Products Using Near-Critical Solvents*, Blackie Academic and Professional, Glasgow, 1993.

4 E. Schutz, *Chem. Eng. Technol.*, 2007, **30**, 685–688.
5 Z. Tang, X. H. Xie and B. N. Zong, *Chinese J. Chem. Eng.*, 2004, **12**, 498–504.
6 Z. Knez and E. Weidner, *Curr. Opin. Solid State Mater. Sci.*, 2003, **7**, 353–361.
7 P. M. Gallagher, M. P. Coffey, V. J. Krukonis and N. Klasutis, *ACS Symp. Ser.*, 1989, **406**, 334–354.
8 D. J. Dixon, G. Luna-Bercenas and K. P. Johnston, *Polymer*, 1994, **35**, 3998–4005.
9 A. O'Neil, C. Wilson, J. M. Webster, F. J. Allison, J. A. K. Howard and M. Poliakoff, *Angew. Chem., Int. Ed.*, 2002, **41**, 3796–3799.
10 C. N. Field, P. A. Hamley, J. M. Webster, D. H. Gregory, J. J. Titman and M. Poliakoff, *J. Am. Chem. Soc.*, 2000, **122**, 2480–2488.
11 E. Reverchon, G. Della Porta, D. Sannino, L. Lisi and P. Ciambelli, *Stud. Surf. Sci. Catal.*, 1998, **118**, 349–358.
12 E. Reverchon, G. Della Porta, D. Sannino and P. Ciambelli, *Powder Technol.*, 1999, **102**, 127–134.
13 E. Reverchon, I. De Marco and G. Della Porta, *J. Supercrit. Fluids*, 2002, **23**, 81–87.
14 E. Reverchon, G. Della Porta, D. A. Di Trolio and S. Pace, *Ind. Eng. Chem. Res.*, 1998, **3**, 952–958.
15 G. J. Hutchings, J. K. Bartley, J. M. Webster, J. A. Lopez-Sanchez, D. J. Gilbert, C. J. Kiely, A. F. Carley, S. M. Howdle, S. Sajip, S. Caldarelli, C. Rhodes, J. C. Volta and M. Poliakoff, *J. Catal.*, 2001, **197**, 232–235.
16 G. J. Hutchings, J. A. Lopez-Sanchez, J. K. Bartley, J. M. Webster, A. Burrows, C. J. Kiely, A. F. Carley, C. Rhodes, M. Hävecker, A. Knop-Gericke, R. W. Mayer, Robert Schlögl, J. C. Volta and M. Poliakoff, *J. Catal.*, 2002, **208**, 197–210.
17 J. A. Lopez-Sanchez, J. K. Bartley, A. Burrows, C. J. Kiely, M. Hävecker, R. Schlögl, J. C. Volta, M. Poliakoff and G. J. Hutchings, *New J. Chem.*, 2002, **26**, 1811–1816.
18 Z.-R. Tang, J. K. Edwards, J. K. Bartley, S. H. Taylor, A. F. Carley, A. A. Herzing, C. J. Kiely and G. J. Hutchings, *J. Catal.*, 2007, **249**, 208–219.
19 Z.-R. Tang, J. K. Bartley, S. H. Taylor and G. J. Hutchings, *Stud. Surf. Sci. Catal.*, 2006, **162**, 219–226.
20 T. Lu, S. Blackburn, C. Dickenson, M. J. Rosseinsky, G. J. Hutchings, S. Axon and G. A. Leeke, *Powder Technol.*, 2009, **188**, 264–271.
21 Z.-R. Tang, C. D. Jones, J. K. W. Aldridge, T. E. Davies, J. K. Bartley, A. F. Carley, S. H. Taylor, M. Allix, C. Dickinson, M. J. Rosseinsky, J. B. Claridge, Z. Xu, M. J. Crudace and G. J. Hutchings, *ChemCatChem*, 2009, **1**, 247–251.
22 M. Haruta, T. Kobayashi, H. Sano and N. Yamada, *Chem. Lett.*, 1987, **16**, 405–408.
23 For a description of gold reference catalysts see *Gold Bull.*, 2003, **36**, 1.
24 S. Vepreck, D.-L. Cocke, S. Kehl and H. R. Oswald, *J. Catal.*, 1986, **100**, 250.
25 G. M. Schwab and S. B. Kanungo, *Z. Phys. Chem.*, 1977, **107**, 109.
26 D. Rangappa, S. Ohara, M. Umetsu, T. Naka and T. Adschiri, *J. Supercrit. Fluids*, 2008, **44**, 441–445.
27 M. Krämer, T. Schmidt a, K. Stöwe, F. Müller, H. Natter and W. F. Maier, *Appl. Catal., A*, 2006, **302**, 257–263.
28 P. A. Wright, S. Natarajan and J. M. Thomas, *Chem. Mater.*, 1992, **4**, 1053.
29 S. B. Kanungo, *J. Catal.*, 1979, **58**, 419.
30 A. A. Mirzaei, H. R. Shaterian, M. Habibi, G. J. Hutchings and S. H. Taylor, *Appl. Catal., A*, 2003, **253**, 499–508.
31 G. J. Hutchings, A. A. Mirzaei, R. W. Joyner, M. R. H. Siddiqui and S. H. Taylor, *Appl. Catal., A*, 1998, **166**, 143–152.
32 P. Porta, G. Moretti, M. Musicani and A. Nardella, *Catal. Today*, 1991, **9**, 211.
33 G. J. Hutchings, A. A. Mirzaei, R. W. Joyner, M. R. H. Siddiqui and S. H. Taylor, *Catal. Lett.*, 1996, **42**, 21–24.
34 E. Reverchon, I. De Marco and E. Torino, *J. Supercrit. Fluids*, 2007, **43**, 126–138.